ORIGINAL ARTICLE

CrossMark

Effects of process parameters on thickness thinning and mechanical properties of the formed parts in incremental sheet forming

Yanle Li [1,2,3] · Xiaoxiao Chen [1] · Weidong Zhai [1] · Liming Wang [1,3] · Jianfeng Li [1,3] · Zhao Guoqun [4]

Abstract

Incremental sheet forming (ISF) is a promising method for forming metal sheets, by which parts can be manufactured without the use of dedicated dies. However, the process has not been widely used for industrial application due to the unsatisfactory service performance of the formed parts. This paper focuses on improving the thickness distribution and mechanical properties (e.g., hardness, yield strength, and tensile strength) through process optimization. The response surface methodology with a Box-Behnken design is used to investigate how different process parameters affect the thickness thinning and mechanical properties. A set of experiments with 15 tests for pyramid-forming process is performed, and three parameters including step-down size, sheet thickness, and tool diameter are considered. The results show that the maximum thinning rate is lower with larger step-down size and larger tools. In addition, compared with the initial sheet, the values of hardness, yield strength, and tensile strength have been increased considerably due to the strain hardening. The present work provides useful guidance in improving the product quality formed by incremental sheet forming.

Keywords Incremental sheet forming · Thickness thinning · Mechanical properties · Hardness · Forming quality

1 Introduction

Incremental sheet forming (ISF) is a promising sheet metal forming process in which no dedicated die is required. During the forming process, the sheet is incrementally deformed by a hemispherical-headed punch that moves following a series of contour lines scattered from a 3D model. The benefits of this forming technology include the reduced forming force, enhanced formability and greater process flexibility suitable for low-series production and specific customer's requirement [1, 2]. The production cycle for ISF is greatly shortened without the production of the forming die. Raju et al. [3] revealed the mechanics for the enhanced formability during the ISF, by investigating the strain distribution condition and the failure mode. In addition, Ambrogio et al. [4] theoretically justified that the formability of material is improved which contributes to the manufacture of complicated parts.

The inadequate geometric accuracy, excessive thickness thinning, and dissatisfied formed mechanical properties of ISF still hindering its wide industrial application [1]. In terms of the geometric accuracy, due to the lack of support, geometric error for ISF currently can only achieve around ± 2 mm while the specification from industrial users are typically within ± 0.2 mm over the whole surface of a part [5]. Strategies including using tool path compensation [6], two moving forming tools [7] and multi-stage forming [8] were adopted with the attempt to improve the geometry accuracy. Lu et al. [9] presented a feedback control strategy to obtain improved geometric accuracy.

Based on the volume conservation theory, thickness thinning happens during ISF since the surface area is increased. In particular, excessive thinning has been an obstacle to the wide application of incremental forming technology. The sine law was used by Kobayashi et al. [10] to predict the final wall thickness by assuming shearing is the main deformation mode

✉ Liming Wang
   liming_wang@sdu.edu.cn

1   Key Laboratory of High Efficiency and Clean Mechanical Manufacture, Ministry of Education, School of Mechanical Engineering, Shandong University, No.17923, Jingshi Rd, Jinan 250061, China

2   State Key Laboratory of High Performance Complex Manufacturing, Central South University, Changsha 410083, China

3   National Demonstration Center for Experimental Mechanical Engineering Education, Shandong University, Jinan 250061, China

4   School of Material Science & Engineering, Shandong University, Jinan 250061, China

in ISF. From this point of view, a vertical flange is unobtainable as the final thickness would be zero. Jeswiet and Young [11] has shown that the maximum formable wall angle for 1.21-mm-thick 3003-O aluminum is 71°. However, a non-uniform wall thinning has been observed. Young and Jeswiet [12] has proved that thickness distribution in ISF process does not always follow the sine law. This is explained by Kegg [13] that an overspinning condition similar to that of shearing forming could occur. Since thinning is a precursor of failure, unexpected failures will take place in the excessive thinning band. Although Kim and Yang [14] and Liu et al. [15] found that multi-pass forming is an effective approach to avoid excessive thinning in specific area, the increased time cost is unsatisfactory. Mirnia et al. [16] used the sequential limit analysis (SLA) to predict the minimum thickness and studied the effect of the tool diameter and the step down on the thickness distribution. Li et al. [17, 18] performed detailed finite element analysis regarding the deformation mechanism in ISF. Methods including response surface method, sequential limit analysis, and finite element analysis were used to predict and optimize thickness distribution [19]. Existing research shows that the tool diameter and step down significantly affect the distribution of wall thickness. Nevertheless, most of these studies are based on simulations and only the effect of a single factor on the minimum thickness has been investigated.

Mechanical properties are key factors for evaluating the product performance before industrial applications. After plastic deformation of metals, grains are gradually squashed or elongated and strain hardening is occurred, resulting in the sharp decrease of plasticity of the material and remarkable increase of the strength. The strain hardening has been studied by many researchers. Tian et al. [20] proposed a method for determining the hardening curve of metal sheets, and Naybi et al. [21] investigated the mechanical properties of steels after heat treatment. The increase of hardness during the strain hardening process has been observed by Rojacz et al. [22]. Fan et al. [23] analyzed the microstructure evolution during electric-assisted incremental forming and found that the grains of original sheet present isotropic distribution while the grains are significantly elongated in the beginning region of formed parts. Similar results were observed by Jeswiet et al. [24] and Ambrogio et al. [25]. Long et al. [26] introduced ultrasonic energy into ISF process and proved to be effective in force reduction. It can be concluded that the incremental forming is an enhanced process for the hardness and the tensile strength due to the high pressure. The above study suggests that the phenomenon of strain hardening does exist, but only qualitative relations between process parameters and mechanical properties were given. Further microcosmic mechanics behind this is required.

Although substantial research work has been conducted on the thickness distribution, the interactive effect of process parameters on minimum thickness by using experiments has had little attention. The relation between process parameters and the minimum thickness as well as its location is usually studied by finite element method. In addition, the mechanical properties of the sheet material after ISF process have not received sufficient attention yet. Therefore, in the present work, experiments with a Box-Behnken design is used to study the interactive effect of process parameters on maximum thinning rate. In particular, mechanical properties including hardness, yield, and tensile strength for the formed parts are focused in this study. The major work is briefly summarized as follows:

- A set of experiments for incremental sheet forming of truncated pyramids was performed by using the response surface methodology (RSM) with a Box-Behnken design. In particular, three independent parameters (step size, sheet thickness, and tool diameter) were varied at three levels to study their effects on maximum thinning rate and mechanical properties of the formed parts.
- Empirical models were developed for predicting the maximum thinning rate by the response function where the effect of each factor on the response is analyzed in detail. In addition, an optimization of the maximum thinning rate was conducted using the desirability function to obtain the optimal working condition.
- The mechanism for the enhanced mechanical properties (hardness, yield strength, and tensile strength) during ISF was discussed. Specifically, the interactive effects of process parameters on mechanical properties of formed parts were studied by response surfaces of experimental results.

2 Methodologies

This section firstly provides the design method of experiments, followed by the procedure description of the acquisition of concerned data including maximum thinning rate and mechanical properties (hardness, yield strength, and tensile strength).

2.1 Design of experiments

The Box-Behnken design is adopted using Minitab software to study the effects of different experimental parameters at different levels on the forming process. Based on previous work, step size, sheet thickness, and tool diameter are selected as the main influencing parameters. Three parameters and their corresponding values are listed in Table 1. Accordingly, 15 experiments are designed according to the number of factors and levels as shown in Table 2.

Table 1 Experimental parameters and levels

Symbols	Factors	Levels		
		− 1	0	1
A	Step size (mm)	0.5	1	2
B	Sheet thickness (mm)	1.27	1.8	2.54
C	Tool diameter (mm)	10	20	30

2.2 Experimental setup

An AMINO machine dedicated for the ISF process was used to deform the flat sheet into designed 3D shape as shown in Fig. 1. The body of hemispherical forming tool is made of K110 steel that was hardened and tempered to HRC60, while its tip is tungsten carbide. No rotation of the tool was allowed in the forming process. Material of the sheet to be processed is 7075-O aluminum alloy, whose size is 300 mm × 300 mm. This material has high strength and good mechanical property and is mainly used for manufacturing of aircraft structures. The target shape of the forming process is truncated pyramids that can obtain flat side wall which is convenient for subsequent measurements. The size of the deformation zone is 150 mm × 150 mm, and the forming angle is 60° with a target forming depth of 65 mm. In this study, three experimental parameters including step size, tool diameter, and sheet thickness were selected as variable of ISF process. The step size is the vertical distance between two neighboring contours, and the wall angle means the angle between the deformed sheets to the horizontal plane.

In order to fix the sheet during forming process, 12 evenly distributed blank holders were used to clamp the sheet to avoid unwanted movement. During the forming process, the forming tool is numerically controlled by a FANUC controller to follow the predesigned tool path. To reduce the friction between the forming tool and sheet, Shell Tellus Oil 68 was used as the lubricant.
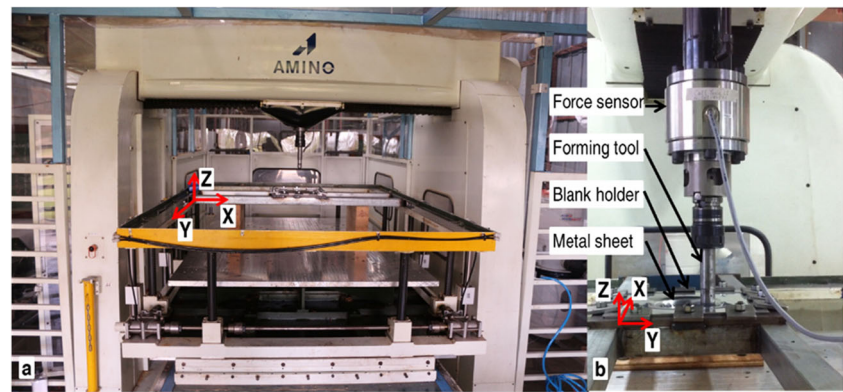
2.3 Measurement of maximum thinning rate

A Kraukramer CL5 ultrasonic thickness gauge was used to measure the thickness of the formed parts. Before measuring the thickness at the deformation zone, calibration was performed to get the propagation velocity of the ultrasonic in the target material. One end of the cable was inserted into the thickness gauge, and the other end was provided with a probe, contacting with the surface at the testing location by the couplant. The thickness measurement was conducted along the vertical direction along the midline of the side wall of the formed pyramid parts. The measurement starts at the forming depth of 10 mm and was taken every 5 mm along the vertical direction for a total of 10 points. For each point, three measurements were taken and the average value was treated as the measured thickness. Since no considerable difference of the thickness was observed among four sides of the same formed part, only one side of one pyramid was selected to take the measurement. Then, the maximum thickness rate of each pyramid part can be calculated as follows:

$$K = \frac{t_0 - t_{min}}{t_0} \times 100\% \tag{1}$$

Table 2 The Box-Behnken design and measured results

Test run no.	A	B	C	Maximum thickness thinning rate (%)	Hardness (HV)	Increase rate of tensile strength (%)	Increase rate of yield strength (%)
1	0	0	0	53.78	48.97	23.12	138.45
2	− 1	0	1	57.22	56.23	25.43	139.56
3	1	1	0	51.30	42.95	19.30	99.54
4	− 1	0	− 1	51.11	54.20	27.56	126.67
5	1	− 1	0	50.31	47.87	27.14	159.63
6	0	− 1	− 1	51.10	52.00	29.78	156.50
7	− 1	− 1	0	54.25	51.55	32.19	170.10
8	0	− 1	1	55.83	56.63	23.24	146.78
9	0	0	0	53.56	48.45	22.59	123.68
10	0	0	0	53.63	48.05	22.27	137.03
11	0	1	− 1	52.31	52.21	21.23	138.54
12	1	0	− 1	50.44	50.87	22.89	124.01
13	0	1	1	56.26	48.30	18.17	146.63
14	− 1	1	0	53.12	56.20	22.67	209.47
15	1	0	1	52.89	49.33	20.76	118.89

Fig. 1 The AMINO incremental forming machine. **a** Front view. **b** Detailed side view

where t_0 is the thickness of initial sheet and t_{min} is the minimum thickness of formed parts.

2.4 Measurement of hardness

The microhardness is an important property that reflects the resistance of a material to the elastoplastic deformation. The microhardness tester MH-6 was used to measure the hardness of the surface for the formed pyramid parts. Testing samples were cut with the size of 40 mm × 40 mm at the same location from the side wall of formed pyramid parts. During the measurement, the load was set as 200 g and the loading time was set as 10 s. Equispaced 9 points were selected at the contact surface to obtain the average value that represents the hardness of one sample.

2.5 Measurement of yield and tensile strength

The tensile test is a widely used experimental method for the determination of mechanical properties for materials. Standard tensile specimens were cut in accordnance with GB/T228.1-2010. Figure 2a shows tensile specimens cut from the initial sheet and the side wall of the formed parts. For the formed parts, the longitudinal direction of the sample is parallel to the tool-forming trajectory and was cut at a distance of 35 mm from the bottom. Specific dimensions of the specimens are shown in Fig. 2b. Tensile specimens were uniformly stretched at a rate of 2 mm/min using a universal testing machine so that the stress-strain curve can be obtained. Since there is no continuous yield platform in aluminum materials,

the stress at the 2% residual deformation is regarded as the yield strength. The maximum stress in the stress-strain curve is regarded as the tensile strength. Then, the obtained yield strength and tensile strength are studied.

3 Experimental results and discussion

In this section, experimental results regarding the effects of processing parameters on the maximum thinning rate and mechanical properties (hardness, yield strength, and tensile strength) are presented and discussed. Specifically, the calculated maximum thinning rate and mechanical properties of each test according to the Box-Behnken design are firstly recorded in Table 2. Then, the effect of each factor on the maximum thinning rate and mechanical property is discussed and analyzed in detail. In addition, regressive models for predicting the maximum thinning rate and material properties are established and the optimized experimental setting for the desired response during pyramid-forming processes is obtained by Minitab.

3.1 Maximum thinning rate

The variation of the sheet thickness along the forming depth is firstly analyzed. One of the formed parts by ISF process (step size 0.5 mm, sheet thickness 1.27 mm and tool diameter 20 mm) is presented in Fig. 3a, and the corresponding thickness distribution is shown in Fig. 3b. Along the depth direction, the sheet thins until it reaches the minimum value and

Fig. 2 Tensile specimens. **a** Prepared specimens. **b** Specific dimensions of the specimen
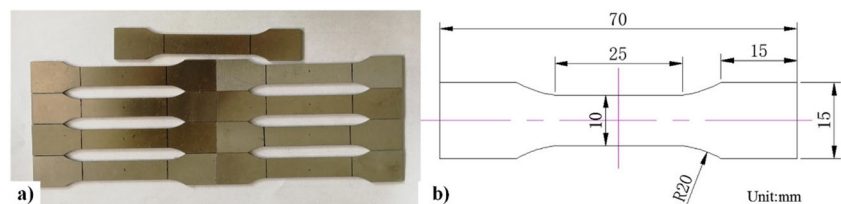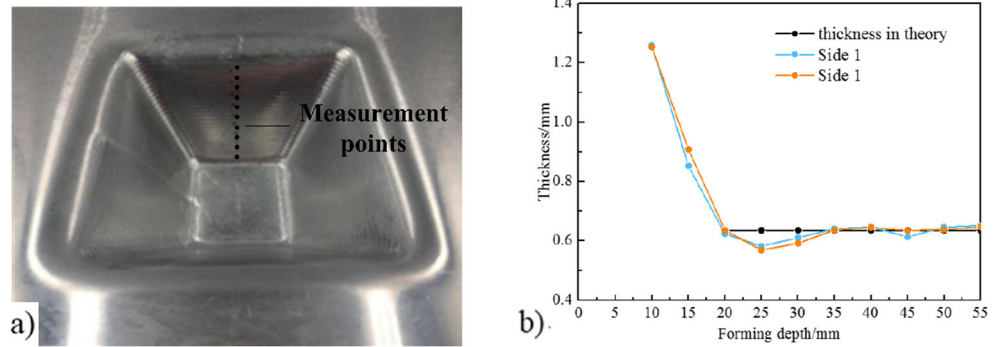
Fig. 3 **a** Measurement points. **b** Thickness distribution of the inclined wall along the forming depth

then it stabilizes around the predicted thickness value by the sine law. This variation trend indicates that an over-spinning condition occurred [21]. The deformation at the initial stage is due to bending while shear deformation takes a considerable portion in the following stages. It is also observed that the minimum thickness always occurs in the forming depth between 25 and 30 mm, which locates at the upper part of the side wall of formed pyramid parts. In addition, as shown in Table 2, the maximum thinning rate is within the range of 50.31–57.22%, larger than the theoretical value (50%) calculated from the sine law.

A regression model for predicting the maximum thinning rate with three process parameters was obtained from Box-Behnken experimental results. To guarantee the fitness and accuracy of the developed response function, the following aspects have to be taken into account. First, the analysis of variance (ANOVA) is adopted to evaluate the importance of each factor to the response and the fitness of the established model. The results of ANOVA for maximum thinning rate are listed in Table 3. Based on a confidence level of 95%, the effect of each factor on the response can be judged as significant if the P value is less than or equal to 0.05. As can be seen from Table 3, among factors that have a linear effect on the maximum

thinning rate, the step size (A) and tool diameter (C) are significant items. Among the factors that have a quadratic effect on the maximum thinning rate, step size (A^2) is a significant item. Among the factors that interactively influence the maximum thinning rate, step size with sheet thickness (AB) and step size with tool diameter (AC) are significant items.

The expression of the response function after removing the non-significant items is shown in formula (2), where the meaning of factors A, B, and C are listed in Table 1. The physical meaning of the formula is that the maximum thinning rate is mainly positively affected by the tool diameter while negatively affected by the step size and quadratic term of step size.

$$K = 53.657 - 1.330A + 2.266C - 1.090A^2 + 0.560AB - 0.915AC \tag{2}$$

Second, residual plot of maximum thinning rate shown in Fig. 4 indicates that the developed model is effective to predict other combination of forming parameters. The residual means the difference between the measured and predicted values. The residuals versus their expected percentiles are shown in the top left image. It is observed that the points are closely distributed around the fitted line, indicating a good fit of the regression model. The histogram in the lower left corner shows that the residual data is approximately a normal distribution, which proves the validity of the model. The residual values of each test are plotted in the right image.
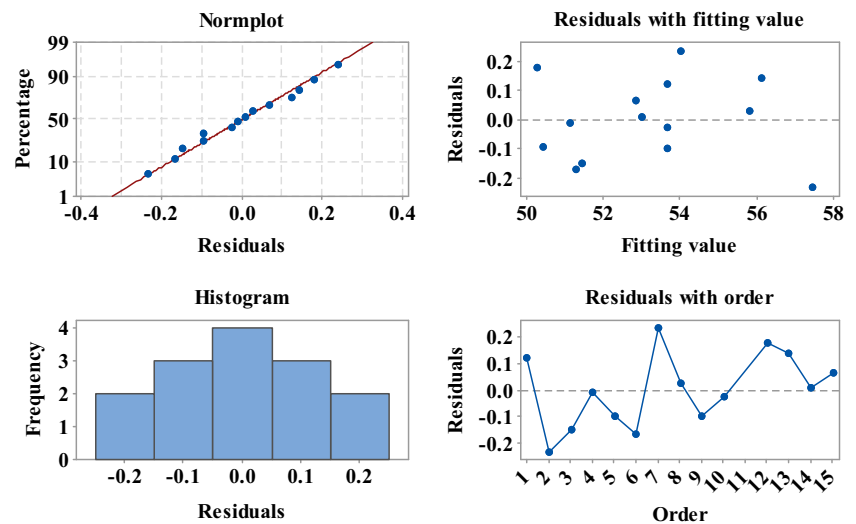
The response surface plots of the maximum thinning rate with the variation of three factors are presented in Fig. 5. In each subfigure, the 3D response surface regarding maximum thinning rate is depicted versus two factors listed in Table 1 while the remaining one is held at the middle level.

Among all experimental cases, the maximum thinning rate can reach up to 57.22% in the worst condition, larger than the theoretical value according to sine law. As shown from Fig. 5b, c, the maximum thinning rate increases with tool diameter, presenting a linear change. In the case of using large tools, it is obvious that the contact area between forming tool and sheet is also large. Then, more material is involved into plastic deformation during a single forming pass. Because of this, the sheet material experienced more forming passes under the

Table 3 Results of ANOVA

Source	F value	P value	Remarks
Model	83.60	< 0.0001	Significant
A	170.76	< 0.0001	Significant
B	0.24	0.174	
C	330.52	< 0.0001	Significant
A^2	42.98	0.003	Significant
B^2	4.49	0.102	
C^2	4.38	0.104	
AB	15.14	0.018	Significant
AC	40.41	0.003	Significant
BC	0.02	0.899	
Lack of fit	12.12	0.076	

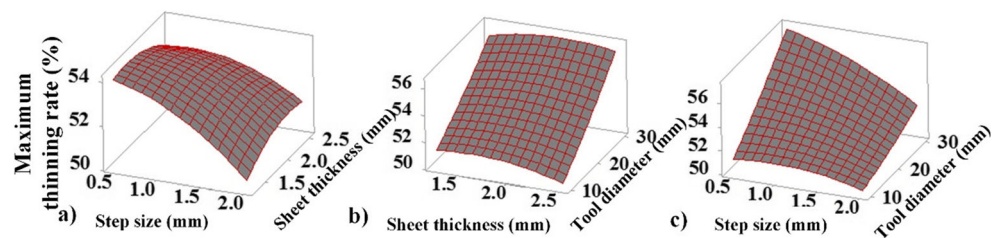**Fig. 4** Residuals of response function for maximum thinning rate

same step-down size, resulting in more obvious material thinning. This is in consistent with the conclusion by Kim and Park [27] in which the effect of tool size on the formability during the straight groove test was analyzed. From Fig. 5a, c, it can be seen that the decrease of the maximum thinning rate appears to be inversely proportional to the rise of step size. Similar to the effect of tool diameter on the response, the number of forming passes for smaller step size is larger than that with larger step size. This is because that the sheet deformation band is narrow under small step size at one single forming pass. Therefore, small step size is more likely to lead to local tensile instability and even fracture. Although the smaller step size and larger tool diameter are helpful for the deformation uniformity, too many times of the deformation should be avoided considering the failure of the material. Due to the interaction effects of AB (step size and sheet thickness) and AC (step size and tool diameter), the slope of the response surface varies with the change of step size, especially when the sheet thickness is small and the tool diameter is large. As indicated in Fig. 5c, the effect of step size on maximum thinning rate is not significant when tool diameter is small, while the same effect is considerable when tool diameter is large. With the increase of step size, the number of tool passes can be decreased. In other words, the effect of tool

diameter can balance the adverse effect of step size on the response. It can be seen from Fig. 5a, b that the effect of sheet thickness on maximum thinning rate is not significant. The response only slightly increases with the increase of a sheet thickness at large step size. This may be due to the interaction of various factors.

The desirability function from Minitab is used to find the optimal combination of process parameters. The aim of the optimization is to find a combination of parameters to minimize the maximum thinning rate. The optimization process and corresponding results are presented in Fig. 6 within the current experimental setting range. The desirability and optimal parameters setting are listed at the first row. The curves present the changing trend of predicted response over the complete experimental range for three factors. The vertical line marked at higher value of desirability is used to find optimal parameter combination. The optimal condition obtained from above analysis is a combination with step size of 2 mm, sheet thickness of 1.27 mm, and tool diameter of 10 mm. The predicted value of the maximum thinning rate is 49.62%. Since the optimized parameters are set at their boundary values, it is suggested that only a local optimization solution is obtained.

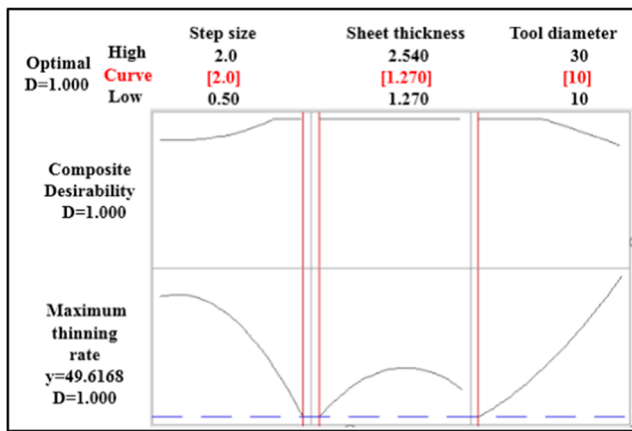**Fig. 5** Response surfaces for maximum thinning rate

Fig. 6 Response optimization results for maximum thinning rate

3.2 Mechanical properties

3.2.1 Hardness

The hardness of the sheet is improved after the ISF process. The hardness of the initial sheet surface is between 28.77–34.16 HV, while the hardness after plastic deformation by ISF is in the range of 48.03–56.23 HV according to the measured results presented in Table 2. The material experienced large plastic deformation during pyramid-forming process, causing significant strain hardening. Strain hardening mainly refers to the phenomenon that hardness and strength of material increase while toughness of material reduces due to the increase of plastic deformation. The reason is that when stress increases until more than one slip system starts at the same time, dislocations intersect with each other so that dislocations are pinned and difficult to move, resulting the increase of strain hardening and hardness.

Similar investigation approach for the maximum thinning rate was used for studying microhardness. The expression of response function is obtained as formula (3), where the hardness is represented by H. A value of 95.47% for R^2 is obtained which means that the obtained model can explain 95.47% changes of response. The effectivity is verified by the residual analysis. It is suggested that microhardness is mainly positively affected by both the linear and quadratic terms of sheet thickness while negatively affected by interactive effect of step size and tool diameter.

$$H = 51.4 + 1.17A + 5.22B - 0.494C + 2.08A^2 + 3.26B^2 + 0.042C^2 \\ - 4.89AB - 0.0917AC - 0.622B \tag{3}$$

Response surfaces shown in Fig. 7 illustrate the effects of step size, sheet thickness, and tool diameter on the surface microhardness. As shown in Fig. 7b, the increase of hardness appears to be linearly proportional to the increase of tool diameter when the sheet thickness is at the middle level. The use of large forming tool will increase the contact area between the forming tool and the sheet, causing that the material suffers repeated squeezing action. This enhances the stress of material and has direct influence on the surface hardness. However, when the sheet thickness is 2.54 mm, the section of response surface with the variation of the tool diameter presents a parabolic trend. The hardness is lowest when a 20-mm forming tool is used. In terms of the effect of sheet thickness, as shown in Fig. 7a, c, the use of thicker sheet results in larger values of hardness. As described in Sect. 3.1, the maximum thinning rate decreases with the increase of step size, which means thick sheet is obtained. To this end, large forming force is required. Therefore, in the condition of the same contact area, the surface of the sheet material withstands large stress, which may lead to the growth of the hardness. In contrast, it can be seen from Fig. 7a, b that the effects of step size on hardness enhancement are not consistent. The use of large step size adversely affects the hardness when the material thickness is below the middle level. However, when sheet thickness is large, the hardness decreases with the rise of step size.

3.2.2 Tensile strength and yield strength

The engineering stress-strain curves are obtained from tensile tests. The tensile strength is defined as the stress corresponding to the maximum load before breaking. Since no obvious physical yield phenomenon occurred in tensile tests of AA7075, the yield strength is defined as the stress with

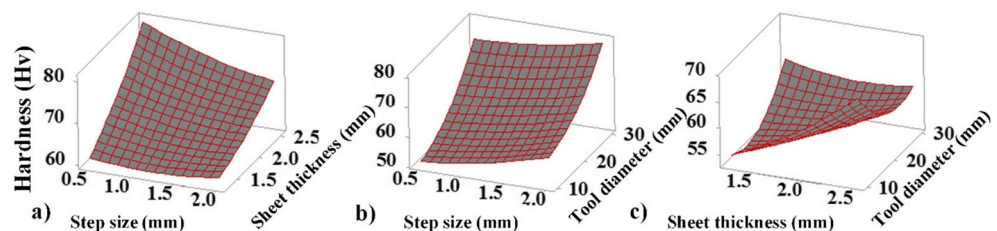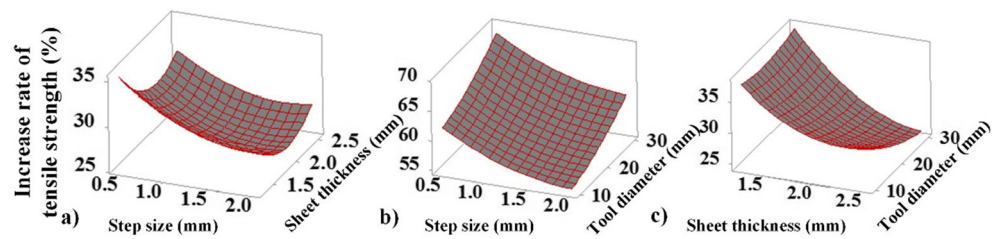**Fig. 7** Response surfaces for microhardness

Fig. 8 Response surfaces for the increase rate of tensile strength

0.2% residual deformation. The tensile strength is analyzed first in this section followed by the yield strength.

Compared to the value of the initial sheet, the tensile strength is increased by a range of 18.17–32.19% so that the carrying capacity of parts is enhanced after incremental forming. It is known that the tensile and yield strength are inherently influenced by the initial sheet thickness. Therefore, in this model, the increase rate of tensile and yield strength are selected as the response to eliminate the influence of the sheet thickness. The response function for tensile strength is expressed as formula (4), where T represents the tensile strength. Similar to the analysis of hardness, a value of 99.79% for R^2 suggests that the developed regression model can explain 99.79% variation of tensile strength within the considered range.

$$T = 66.3 - 11.6A - 29.74B - 0.012C + 2.78A^2 + 6.99B^2 + 0.00842C^2 \\ - 0.909AB - 0.243B \tag{4}$$

In Fig. 8, response surfaces are given to reveal how factors affect the increase rate of tensile strength. From Fig. 8a. b, it can be concluded that the increase rate of tensile strength decreases with the increase of step size. For one reason, the large step size reduces the total forming passes of the process therefore the material experiences less contact with the forming tool than that of using small step size. For another, the large step size causes a non-uniform flow of metal material. The internal surface topography at this condition shows that there are obvious track marks on the formed surface, which weaken the deformation reinforcement. Therefore, the rate of enhancement for tensile strength decreases with large step size. Figure 8b, c shows that the increase rate of tensile strength grows with the increase of tool diameter when sheet

thickness is at middle level. The increase of tool diameter results in a large contact area between the sheet and the forming tool, and more metal material is involved into deformation in a single forming pass. To this end, a uniform plastic deformation can be obtained. The influence of the sheet thickness on the response is presented in Fig. 8a, c. Since the designed shape is formed from one side of sheet, the squeezing action of the tool decreases along the sheet thickness direction. Therefore, thick sheet thickness causes insufficient deformation on the non-contact side of the sheet. Consequently, the ability of overall deformation reinforcement is weakened and the increase rate of tensile strength decreases. It is also shown that the effect of sheet thickness and that of tool diameter on the increase rate of tensile strength is opposite. When sheet thickness is small, tool diameter is the dominant factor while sheet thickness is the dominant factor when sheet thickness is large.

In terms of the enhancement of yield strength, an increasing rate range between 99.34 and 209.47% was achieved for the formed parts. The response function for yield strength is expressed as formula (5), where Y represents the yield strength. The residual plot of yield strength was also checked which suggests that obtained regression model is credible.

$$Y = 211 + 237A - 311B + 10.1C - 58A^2 + 158B^2 + 0.287C^2 \\ - 55.7AB - 0.6AC - 11.5BC \tag{5}$$

It can be seen from Fig. 9b, c that the increase rate of yield strength grows with the increase of the tool diameter when the sheet thickness is below 1.8 mm. In Fig. 9a, the increase rate

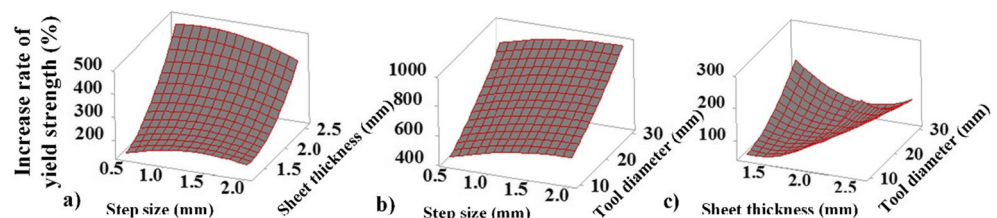**Fig. 9** Response surfaces for the increase rate of yield strength

Table 4 The effect of each factor on four responses

Factors	Maximum thinning rate	Hardness	Tensile strength	Yield strength
Step size(increase)	Decrease	Non-consistent	Decrease	Non-significant
Sheet thickness(increase)	Non-significant	Increase	Non-consistent	Increase
Tool diameter(increase)	Increase	Increase	Increase	Increase

of yield strength increases significantly with the increase of sheet thickness. Since plastic deformation firstly occurs in grains with favorable orientation, the increased stress results in more grains involved into deformation. However, the plastic deformation for all grains is not simultaneous and uniform. This feature can be aggravated with the increase of sheet thickness. Therefore, it is difficult to yield for the thick sheet material. In the contrary, as can be seen in Fig. 9a, b, the effect of step size on the yield strength is not significant.

4 Conclusions

The effects of three process parameters on the maximum thinning rate and mechanical properties (hardness, tensile, and yield strength) were investigated by performing a Box-Behnken design with 15 experiments. Response surface method was successfully applied to analyze both single and interactive influences of step size, tool diameter, and sheet thickness on the selected responses during pyramid-forming processes. Regressive models have been established considering both linear and quadratic effects of most influential forming parameters. Due to the large plastic deformation during the ISF process, values of hardness, tensile, and yield strength after forming were increased remarkably. The effects of three factors on each response are summarized in Table 4, and the main conclusions are also presented.

- The optimum working condition is determined by using desirability function, with the aim of decreasing the maximum thinning rate. It was found that increasing step size or decreasing tool diameter with a limited range is an effective approach to reduce the maximum thinning rate.
- The hardness of the sheet is improved after the ISF process. In particular, the surface micro-hardness can be heavily enhanced by adopting large tool diameter and thick sheet material. By contrast, the effects of step size on hardness enhancement are not consistent.
- The tensile strength for all the measured tests increased by a range of 18.17 to 32.19% compared to the value of initial sheets. The increase of tool diameter and the decrease of step size cause growing in the increase rate of tensile strength. The effect of sheet thickness and that of tool

diameter on the increase rate of tensile strength is opposite.

- In terms of the enhancement of yield strength, an experimentally increasing rate of 99.34 to 209.47% was achieved after incremental forming. The increase rate of yield strength grows with the increase of sheet thickness significantly, but the effect of step size on the yield strength is not significant.
- Suggestions for future investigation are provided.
- To comprehensively evaluate the forming quality of the formed parts, indicators such as fatigue performance and residual stress are also essential.
- In this study, the effects of three main forming parameters (step size, tool diameter, and thickness) are investigated. The effects of parameters such as feed rate, tool rotation speed, wall angle, and tool path strategy are also of interest.

Publisher's Note Springer Nature remains neutral with regard to jurisdictional claims in published maps and institutional affiliations.

References

1. Emmens WC, Sebastiani G, Van den Boogaard AH (2010) The technology of incremental sheet forming—a brief review of the history. J Mater Process Technol 210(8):981–997
2. Li Y, Chen X, Liu Z, Sun J, Li F, Li J, Zhao G (2017) A review on the recent development of incremental sheet-forming process. Int J Adv Manuf Technol 92:2439–2462
3. Raju C, Haloi N, Sathiya Narayanan C (2017) Strain distribution and failure mode in single point incremental forming (SPIF) of multiple commercially pure aluminum sheets. J Manuf Process 30:328–335
4. Ambrogio G, Filice L, Fratini L, Micari L (2004) Process mechanics analysis in single point incremental forming. Columbus. Ohio, USA:AIP Conference Proceedings 922(712): 922–927
5. King JM, Allwood GPF, Duflou J (2005) A structured search for applications of the incremental sheet-forming process by product segmentation. Proc Inst Mech Eng B 219(2):239–244
6. Essa K, Hartley (2011) An assessment of various process strategies for improving precision in single point incremental forming. Int J Mater Form 4(4):401–412

7. Meier H, Magnus C, Smukala V (2011) Impact of superimposed pressure on dieless incremental sheet metal forming with two moving tools. CIRP Ann Manuf Technol 60(1):327–330

8. Bambach M, Taleb Araghi B, Hirt G (2009) Strategies to improve the geometric accuracy in asymmetric single point incremental forming. Prod Eng 3(2):145–156

9. Lu H, Michael K, Li Y, Liu S, Daniel WJT, Meehan PA (2016) Model predictive control of incremental sheet forming for geometric accuracy improvement. Int J Adv Manuf Technol 82(9–12):1781–1794

10. Kobayashi S, Hall IK, Thomsen EG (1961) A theory of shear spinning of cones. Tran ASME, J Eng Indust 83:485–495

11. Jeswiet J, Young D (2005) Forming limit diagrams for single point incremental forming of aluminium sheet. Proc Inst Mech Eng B 219(4):359–364

12. Young D, Jeswiet J (2004) Wall thickness variations in single point incremental forming. Proc Inst Mech Eng B 218(B11):204–210

13. Kegg Richard L (1961) A new test method for determination of spinnability of metals. J Eng Ind-T ASME 83(2):119–124

14. Kim TJ, Yang DY (2000) Improvement of formability for the incremental sheet metal forming process. Int J Mech Sci 42(7):1271–1286

15. Liu B, Daniel WJT, Li Y, Liu S, Meehan PA (2014) Multi-pass deformation design for incremental sheet forming: analytical modeling, finite element analysis and experimental validation. J Mater Process Technol 214(3):620–634

16. Mirnia MJ, Dariani BM, Vanhove H, Duflou JR (2014) An investigation into thickness distribution in single point incremental forming using sequential limit analysis. Int J Mater Form 7(4):469–477

17. Li Y, Daniel WJT, Meehan PA (2017) Deformation analysis in single-point incremental forming through finite element simulation. Int J Adv Manuf Technol 88:255–267

18. Li Y, Daniel WJT, Liu Z, Lu H, Meehan PA (2015) Deformation mechanics and efficient force prediction in single point incremental forming. J Mater Process Technol 221:100–111

19. Behera AK, de Sousa RA, Ingarao G, Oleksik V (2017) Single point incremental forming: an assessment of the progress and technology trends from 2005 to 2015. J Manuf Process 27:37–62

20. Tian H, Kang D (2003) A study on determining hardening curve for sheet metal. Int J Mach Tools Manuf 43(12):1253–1257

21. Nayebi A, Bartier O, Mauvoisin G (2001) Abdi R EI. New methods to determine the mechanical properties of heat treated steels. Int J Mech Sci 43(11):2679–2697

22. Rojacz H, Mozdzen G, Winkelmann H (2014) Deformation and strain hardening of different steels in impact dominated systems. Mater Charact 90:151–163

23. Fan G, Li G (2014) Mechanical property of Ti-6Al-4V sheet in one-sided electric hot incremental forming. Int J Adv Manuf Technol 72(5–8):989–994

24. Jeswiet J, Micari F, Hirt G, Bramley A, Duflou J, Allwood J (2005) Asymmetric single point incremental forming of sheet metal. CIRP Ann Manuf Technol 54(2):623–649

25. Ambrogio G, Gagliardi F, Bruschi S, Filice L (2013) On the high speed single point incremental forming of titanium alloys. CIRP Ann Manuf Technol 62(1):243–246

26. Long Y, Li Y, Sun J, Ille I, Li J, Twiefel J (2018) Effects of process parameters on force reduction and temperature variation during ultrasonic assisted incremental sheet forming process. Int J Adv Manuf Technol 97(1–4):13–24

27. Kim YH, Park JJ (2002) Effect of process parameters on formability in incremental forming of sheet metal. J Mater Process Technol 130:42–46